

## The effect of peptone on the structure of electrodeposited Sn-Fe binary alloys

G. B. Lak<sup>1</sup> · L. Sziráki<sup>2</sup> · E. Kuzmann<sup>2</sup> ·  
S. Stichleutner<sup>2,3</sup> · C. U. Chisholm<sup>1</sup> · M. El-Sharif<sup>1</sup> ·  
G. Varga<sup>4</sup> · K. Havancsák<sup>4</sup> · Z. Homonnay<sup>2</sup>

© Springer International Publishing Switzerland 2016

**Abstract** Sn-Fe thin films were electrodeposited by constant current deposition on copper substrates using an aqueous gluconate based electrolyte with varying concentrations of the organic additive peptone. Good quality metallic deposits were obtained with surface morphologies which varied with the concentration of peptone present in the electrolyte. The effect of peptone concentration on the deposition process was studied using electrochemical polarization curves and EDX analysis. The effect of peptone concentration on deposit structure and surface morphology was investigated by X-ray diffraction (XRD), scanning electron microscopy (SEM) and <sup>57</sup>Fe and <sup>119</sup>Sn conversion electron Mössbauer spectroscopy (CEMS). It was concluded that the addition of small amounts of peptone to the electrolyte slightly increased the bath stability and led to changes in the alloy composition of the electrodeposits. It was found that increases in the peptone content increased the amount of the crystalline structure in the deposits with corresponding reductions in the amounts of amorphous structure present in the deposits.

**Keywords** Amorphous alloys · Sn-Fe binary alloys · Electroplating · Electrochemical properties · Mössbauer spectroscopy · X-ray diffraction · Scanning electron microscopy (SEM) · Energy dispersive microanalysis of X-ray (EDX)

---

This article is part of the Topical Collection on *Proceedings of the International Conference on the Applications of the Mössbauer Effect (ICAME 2015), Hamburg, Germany, 13-18 September 2015*

---

✉ E. Kuzmann  
Kuzmann@caesar.elte.hu

<sup>1</sup> Glasgow Caledonian University, 70 Cowcaddens Road, Glasgow, G4 0BA, UK

<sup>2</sup> Institute of Chemistry, Pázmány Péter sétány 1/A, Eötvös Loránd University, Budapest, 1117, Hungary

<sup>3</sup> Centre for Energy Research, Hungarian Academy of Sciences, Konkoly Thege Miklós út 29-33, Budapest, 1121, Hungary

<sup>4</sup> Institute of Physics, Pázmány Péter sétány 1/A, Eötvös Loránd University, Budapest, 1117, Hungary

## 1 Introduction

Tin and tin based alloy deposition is highly sensitive to the electrolyte parameters, such as pH and additives. Several different inorganic and organic additives are in development currently for leveling, brightening, reducing stress and improving the bath throwing power in the case of tin deposition [1–4]. In order to get bright metallic fine grained compact deposits, it has been found necessary to use the additive peptone in electrolytes. In our previous studies we have established that as little as  $0.1 \text{ g dm}^{-3}$  peptone concentration gave deposition of good quality metallic electrodeposited alloys of Fe-Co [5], Sn-Fe, Sn-Co-Fe [6, 7], and Sn-Ni-Fe [8], resulting in mainly amorphous structures. To further examine the effect of small increases in the peptone concentration in the gluconate based electrolyte the binary Sn-Fe electrodeposition system was chosen to facilitate examination of potential fundamental changes in the structure of the alloys brought about by the addition of peptone over a narrow concentration range including the electrolyte system with no peptone for comparative analysis. Based on earlier studies we were of the opinion that small additions of peptone could contribute to the tailoring of the morphology, the alloy composition and the deposit structure of the Sn-Fe alloy deposits giving controlled functional properties.

## 2 Experimental

Sn-Fe thin films were electrodeposited by constant current deposition technique onto copper substrates using an aqueous gluconate based electrolyte (Table 1) with varying concentrations of the organic additive peptone (0, 0.1 and  $0.2 \text{ g dm}^{-3}$ ). The electrolyte solutions were prepared with analytical grade chemicals and Millipore water (specific resistivity  $18 \text{ M}\Omega \text{ cm}$ ) with a  $\text{pH}=5$ . The peptone was purchased from Sigma Aldrich (cat. no. 82962-F). The polarization measurements and the plating were performed in a 2-compartment cell with magnetic probe agitation, and equipped with a Luggin capillary using a saturated calomel reference electrode. The plating cell was thermostatically controlled at  $20 \text{ }^\circ\text{C}$ . High density carbon anodes were placed parallel at the same distance from the cathode. The experimental arrangement was the same as that described previously [8]. The cathode substrates were freshly electropolished  $0.2 \text{ mm}$  thick copper plates with a plated surface area of  $4 \text{ cm}^2$ . The electropolishing pretreatments were made in phosphoric acid solution in advance at a constant potential of  $+1.05 \text{ V vs SCE}$  for 2 minutes. The duration of the galvanostatic electrolysis was 15 minutes. The polarization measurements and the deposition were repeated three times with good reproducibility. The results presented in this paper were obtained with samples from of the 3<sup>rd</sup> plating series.

SEM measurements and the EDX determination of the elemental composition were carried out with a FEI Quanta 3D high resolution scanning electron microscope.

Powder X-ray diffractograms of the samples were measured in Bragg-Brentano geometry using a DRON-2 computer controlled diffractometer (at  $45 \text{ kV}$  and  $35 \text{ mA}$ ) using the  $\beta$  filtered  $\text{FeK}_\alpha$  radiation ( $\lambda = 1.93735 \text{ \AA}$ ) at room temperature. The goniometer speed chosen was  $1/4 \text{ deg min}^{-1}$  in the range of  $2\Theta = 20 - 70 \text{ deg}$ . The diffraction patterns were evaluated using EXRAY peak searching software (developed by Z. Klencsár at the Eötvös University, 1996). For identification of the phases the ASTM X-ray Diffraction Data were used.

$^{57}\text{Fe}$  and  $^{119}\text{Sn}$  conversion electron Mössbauer spectra of the samples were recorded with conventional Mössbauer spectrometers (WISSEL) working in constant acceleration mode

**Table 1** Bath composition used for the Sn-Fe electrodeposits

Component	Sn-Fe c/ mol dm <sup>-3</sup>
SnSO <sub>4</sub>	0.02
FeSO <sub>4</sub>	0.02
NaC <sub>6</sub> H <sub>11</sub> O <sub>7</sub>	0.2
H <sub>3</sub> BO <sub>3</sub>	0.45
NaCl	0.3
C <sub>6</sub> H <sub>8</sub> O <sub>6</sub>	0.01

at room temperature. The conversion electrons were detected by a flowing gas RANGER type detector using He-4 %CH<sub>4</sub> gas mixture. A 50 mCi activity <sup>57</sup>Co/Rh and a 16 mCi activity Ca<sup>119m</sup>SnO<sub>3</sub> sources supplied the gamma rays for <sup>57</sup>Fe and <sup>119</sup>Sn measurements, respectively. The velocity calibration was performed by  $\alpha$ -Fe measurement. The isomer shifts are given relative to  $\alpha$ -Fe and CaSnO<sub>3</sub> for <sup>57</sup>Fe and <sup>119</sup>Sn spectra, respectively. The evaluations of the Mössbauer spectra were made by least square fitting of Lorentzian lines using the MOSSWINN software [9].

### 3 Results and discussion

Potentiodynamic cathodic polarization cycles obtained for Sn-Fe alloys plated at different peptone concentrations can be seen on Fig. 1a. The arrows at the base of the polarization curves show the initiation point for alloy nucleation in each case. The encircled numbers on curves 1-3 illustrate the average potential/deposition current density during each 15 minute galvanostatic deposition. The deposition potential of Sn-Fe alloys with peptone additions begins at a more negative potential of about 0.1 V compared to the alloy deposition with no peptone. This shift can most likely be associated with the increase of the nucleation overpotential. In the case of the electrolyte without any peptone addition, the deposition potential continuously shifts with deposition time to a less negative potential (curve 1 on Fig. 1b). In the presence of peptone, the deposition potentials during galvanostatic deposition are stable for about 5 minutes and thereafter continuously shift to less negative values. This can be explained by increases in the surface area of the deposits, which in turn can lead to decreases of the current density and a shift of the potential.

Plating conditions and composition of the Sn-Fe alloys obtained by EDX analysis are presented in Table 2. The lower deposition potential in the presence of peptone is most probably related to improvements of the throwing power of the electrodeposition process, i.e. with the secondary current density distribution. The composition of the binary alloy deposits significantly changed due to peptone additions, leading to increases in the Sn content with corresponding decreases in the Fe content. A similar tendency for changes in partial currents was observed for individual Sn and Fe deposition when the partial current of Sn increased while that of Fe decreased due to the addition of 0.1 g dm<sup>-3</sup> peptone. Figure 2a-b shows that the estimated deposit thickness and the partial currents of the metal components remain almost the same at 0.1 and 0.2 g dm<sup>-3</sup> peptone concentrations, and the Sn:Fe ratio was found to be around 2:1. It is considered that this may in fact lead to segregation of FeSn<sub>2</sub> phase.

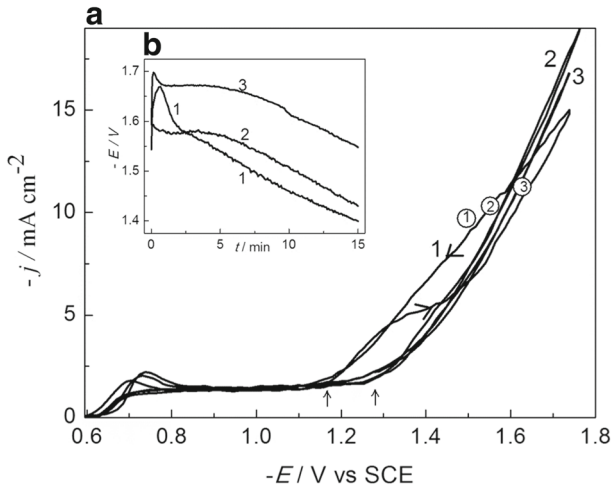


**Fig. 1** **a:** cathodic potentiodynamic cycles obtained for Sn-Fe alloy plated on copper substrate at scan rate  $v = 0.01 \text{ V s}^{-1}$  (2<sup>nd</sup> cycles) at different peptone concentrations: **1)** 0, **2)** 0.1, **3)** 0.2  $\text{g dm}^{-3}$ ; **b:** change of the cathode potential with time of deposition over the same range of peptone concentrations

SEM micrographs (Fig. 3) show the deposits exhibiting a typically coarse dendritic growth morphology, which is enhanced with increasing peptone concentration. This type of growth mode tends to result in a relatively uniform distribution of the alloy components, which was confirmed by the EDX analysis of the Sn and Fe content showing to vary by 0.5-1 % across the range of sites measured. This is probably related to the formation of an intermetallic phase. Peptone, due to its slow adsorption-desorption rate, hinders the rate of diffusion of the alloy components at the catholyte/substrate interface and thus enhances the crystal-growth rate at the expense of the nucleation. Without peptone addition the deposits exhibited a matte grey surface with the edges of the deposit showing poor quality porous powdered structure. With peptone present the deposit surface was found to be smooth and bright, but it became greyish matte in appearance when the deposit thickness increased to more than  $1 \mu\text{m}$ .

Bright, metallic Sn-Fe alloy deposits showing an irregular nodular growth morphology were earlier reported [10] from a gluconate based electrolyte with a Sn:Fe ratio of 1:3 at  $0.1 \text{ g dm}^{-3}$  peptone. These deposits were obtained using a static electrolyte at  $60^\circ\text{C}$  with a current density of  $-25 \text{ mA cm}^{-2}$  resulting in mainly amorphous structures in association with small quantities of crystalline  $\text{FeSn}_2$  and  $\beta\text{-Sn}$ . The extent of the intermetallic  $\text{FeSn}_2$  and tin phase somewhat increased with the thickness of deposits in the  $3\text{-}17 \mu\text{m}$  range. Resulting from the previous work on the alloy deposition, we believe that the amorphous structure and bright appearance of deposits were due to the occlusion of C and O in the growing deposits resulting from the reduction of gluconate at high current density and temperature. It is also important to remember that the results reported in this paper for the Sn-Fe alloy deposition at  $20^\circ\text{C}$  with different peptone concentrations and no peptone present also have a range of electrolyte and process variables which ultimately contribute to the final alloy composition, morphology and structure and hence it is not surprising that earlier studies where electrolyte and process variables were different from those in this study gave results varying from those obtained in the current study.

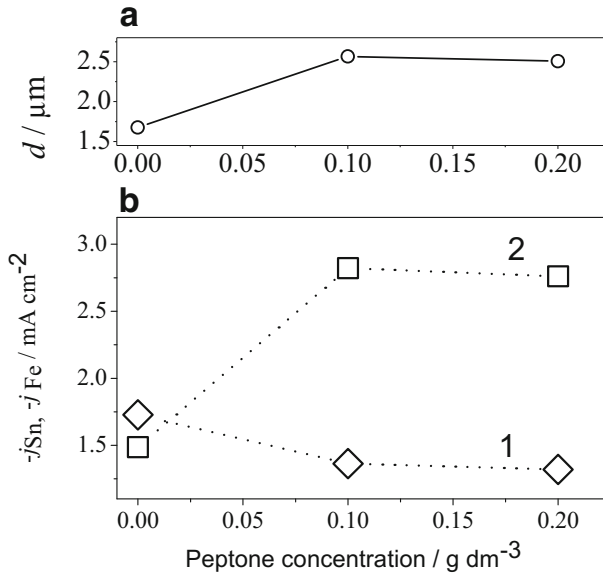


**Fig. 2** a: thickness of the Sn-Fe coatings; b: partial deposition currents of alloy components at different peptone concentrations: 1) Fe, 2) Sn

X-ray diffractograms of the binary Sn-Fe deposits (Fig. 4) exhibit dominant crystalline phases alongside the contribution from peaks belonging to the copper substrate. The XRD pattern of the binary deposit without peptone (Fig. 4a) reveals peaks of major crystalline phases of  $\text{Fe}_{13}\text{Sn}_4$  and  $\text{FeSn}_2$  with a minor amorphous contribution. In the diffractogram of the binary deposit with 0.1  $\text{g dm}^{-3}$  peptone (Fig. 4b) only the crystalline  $\text{FeSn}_2$  phase could be identified, while the binary deposit with 0.2  $\text{g dm}^{-3}$  peptone (Fig. 4c) also has  $\beta$ -Sn present alongside the crystalline  $\text{FeSn}_2$  phase in this deposit. Similar ranges of phases but with different ratios have been reported in earlier studies of binary Sn-Fe deposition [5–7].

The  $^{57}\text{Fe}$  and  $^{119}\text{Sn}$  conversion electron Mössbauer spectra of the binary Sn-Fe samples are displayed in Fig. 5. In accordance with its X-ray diffractogram, the  $^{57}\text{Fe}$  Mössbauer spectrum of the binary deposit without peptone (Fig. 5a) shows a dominant crystalline  $\text{FeSn}_2$  phase together with paramagnetic and ferromagnetic amorphous Sn-Fe alloy phases reflected by a singlet, a doublet and a sextet, respectively. The Mössbauer parameters of the subpectra correspond well to those reported earlier [10]. The  $^{119}\text{Sn}$  Mössbauer spectrum of binary deposit without peptone (Fig. 5b) can be decomposed into a dominant doublet, representing mainly the crystalline  $\text{FeSn}_2$  phase, and a broad magnetically split sextet, reflecting the amorphous Sn-Fe alloy phase, thus complementing the  $^{57}\text{Fe}$  Mössbauer and XRD data for these alloys.

The same components can be fitted in the  $^{57}\text{Fe}$  Mössbauer spectrum of the binary deposit with 0.1  $\text{g dm}^{-3}$  peptone (Fig. 5c) as were found in the spectrum of the binary deposit without peptone. However, the spectrum of the binary deposit with 0.1  $\text{g dm}^{-3}$  peptone does display a further increase in the relative amount of the crystalline  $\text{FeSn}_2$  phase at the expense of the amorphous components. This considerable increase is clearly reflected in the

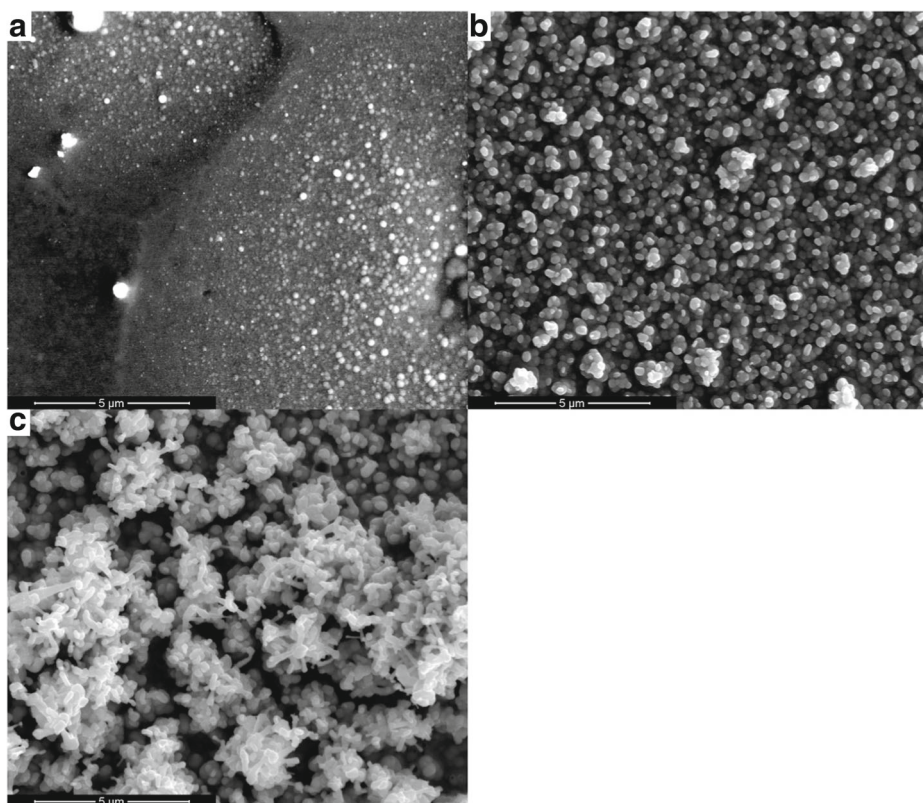


**Fig. 3** SEM micrographs of Sn-Fe alloy deposits plated at different peptone concentrations: a) 0, b) 0.1, c) 0.2 g dm<sup>-3</sup>

<sup>119</sup>Sn Mössbauer spectrum (Fig. 5d) containing a sole doublet component reflecting mainly the FeSn<sub>2</sub> phase. These changes are in a good agreement with the ones observed from the XRD results for the alloy deposits.

No ferromagnetic component could be observed in the <sup>57</sup>Fe Mössbauer spectrum of binary deposit with 0.2 g dm<sup>-3</sup> peptone (Fig. 5e). Both, the <sup>57</sup>Fe and <sup>119</sup>Sn Mössbauer (Fig. 5f) spectra indicate that the crystalline FeSn<sub>2</sub> is the major phase occurring in this deposit. Additionally, a minor singlet component, representing β-Sn [11], could also be identified in the <sup>119</sup>Sn Mössbauer spectrum of the sample, which again was in accordance with the XRD data.

In accordance with the electrochemical and morphological characterization the results of the XRD and Mössbauer measurements of the binary Sn-Fe electrodeposits show a gradual change in the structure and phase composition from a partly amorphous state to a fully crystalline one with increasing peptone concentration in the gluconate electrolyte. This is clearly reflected not only by the XRD results, but also by the total disappearance of the amorphous component and the development of a dominant crystalline FeSn<sub>2</sub> phase in the Mössbauer spectra of the deposits obtained with 0.2 g dm<sup>-3</sup> of peptone. This effect can be attributed to the hindrance of iron deposition with increasing peptone concentration in the binary Sn-Fe system as can be seen in Table 2.

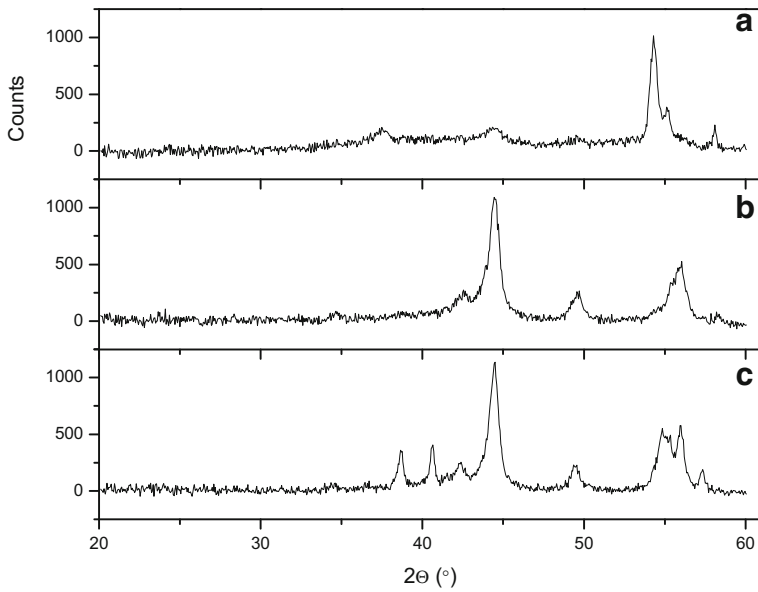


**Fig. 4** XRD diffractograms of binary Sn-Fe deposits plated at different peptone concentrations: **a**) 0, **b**) 0.1, **c**) 0.2 g dm<sup>-3</sup>

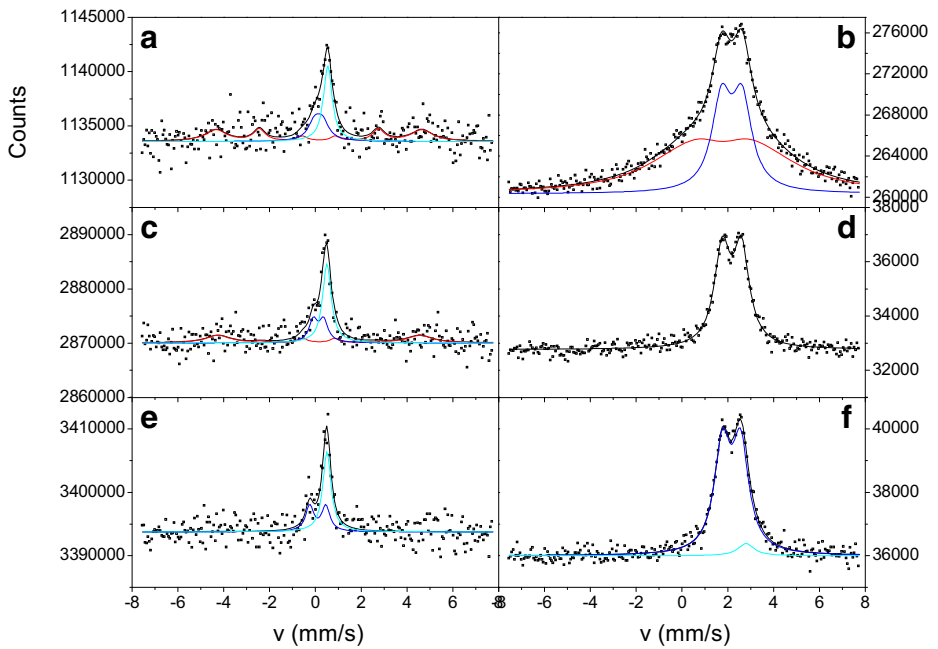


**Fig. 5** <sup>57</sup>Fe (**a,c,e**) and <sup>119</sup>Sn (**b,d,f**) CEM spectra of binary Sn-Fe deposits plated at different peptone concentrations: **a,b**) 0; **c,d**) 0.10; **e,f**) 0.20 g dm<sup>-3</sup>

**Table 2** Plating parameters and average composition of Sn-Fe electrodeposits by EDX analysis

Plating current density/ mA cm <sup>-2</sup>	Average deposition potential/ V	Peptone concentration/ g dm <sup>-3</sup>	Current efficiency/ %	Sn /at %	Fe/ at %
-9.71	-1.496	0	33.10 <sup>1</sup>	46.25	53.75
-10.32	-1.552	0.10	40.55	67.41	32.59
-11.25	-1.628	0.20	36.27	67.66	32.34

<sup>1</sup>estimated minimum value

## 4 Conclusions

Electrochemical polarization characterization, XRD, EDX, SEM and CEMS results for the binary Sn-Fe deposits obtained by constant current deposition on copper substrates using an aqueous gluconate based electrolyte with a range of different peptone concentrations led to the following conclusions. In the binary gluconate based Sn-Fe bath the addition of peptone increases the deposition overvoltage leading to more adherent compact deposits most likely due to the improved secondary current distribution. Peptone additions significantly influence the composition and microstructure of the Sn-Fe electrodeposits up to a concentration ratio of 2:1, but further changes in current efficiency and composition were found to be insignificant. The peptone adsorption on the deposit surface reduces the Fe deposition rate and consequently enhances uniform dendritic crystal growth. Peptone significantly influences the amorphous character of the deposits by changing the chemical short range ordering enhancing the formation of crystalline phases. At the highest peptone concentration of 0.2 g dm<sup>-3</sup> the deposits become fully crystalline without any amorphous phase present.

**Acknowledgments** Financial support from the Hungarian National Research Fund (OTKA project No K68135 K115913) is gratefully acknowledged. The Project is supported by the European Union and co-financed by the European Social Fund (grant agreement no. TAMOP 4.2.1/B-09/1/KMR-2010-0003).

## References

- Jordan, M.: The electrodeposition of tin and its tin-alloys. E.G. Leuze Publishers. D-88348 Saulgau/Württ, 1995
- Lin, K.-L., Chang, J.-T.: The composition and microstructure of electrodeposited solder on electroless nickel in the presence of gelatin. *J Mater. Sci* **30**, 1879 (1995)
- Nakamura, Y., Kaneko, N., Nezu, H.: Surface morphology and crystal orientation of electrodeposited tin from acid stannous sulfate solutions containing various additives. *J Appl. Electrochem* **24**, 569 (1994)
- Kaneko, N., Shinohara, N., Nezu, H.: Effects of aromatic carbonyl compounds on the surface morphology and crystal orientation of electrodeposited tin from acid stannous sulfate solutions, *Electrochim. Acta* **37**, 2403 (1992)
- Chisholm, C.U., Kuzmann, E., Doyle, O., El-Sharif, M., Stichleutner, S., Homonnay, Z., Solymos, K., Vértes, A.: Mössbauer and XRD investigation of electrodeposited Fe, Co and Fe-Co alloys using a gluconate plating process. *J Radioanal. Nucl. Chem* **266**, 533 (2005)



6. Chisholm, C.U., Kuzmann, E., El-Sharif, M., Doyle, O., Stichleutner, S., Solymos, K., Homonnay, Z., Vértes, A.: Preparation and characterisation of electrodeposited amorphous Sn–Co–Fe ternary alloys. *Appl. Surf. Sci.* **253**, 4348 (2007)
7. El-Sharif, M., Chisholm, C.U., Kuzmann, E., Sziráki, L., Stichleutner, S., Homonnay, Z., Süvegh, K., Vértes, A.: The structure and composition of novel electrodeposited Sn–Fe and Sn–Co–Fe alloys from a flow circulation cell system. *Hyperfine Interact.* **192**, 1 (2009)
8. Sziráki, L., Kuzmann, E., El-Sharif, M., Chisholm, C.U., Stichleutner, S., B.Lak, G., Süvegh, K., Tatár, E., Homonnay, Z., Vértes, A.: Electrodeposition of novel Sn–Ni–Fe ternary alloys with amorphous structure. *Appl. Surf. Sci.* **256**, 7713 (2010)
9. Klencsár, Z., Kuzmann, E., Vértes, A.: User-friendly software for Mössbauer spectrum analysis. *J. Radioanal. Nucl. Chem.* **210**, 105 (1996)
10. Chisholm, C.U., El-Sharif, M., Kuzmann, E., Stichleutner, S., Homonnay, Z., Vértes, A.: Electrodeposition of Sn–Fe alloys using gluconate electrolytes and X-ray diffractometry and Mössbauer studies of the deposits. *Mater. Chem. Phys.* **120**, 558 (2010)
11. Stevens, J.G., Stevens, V.: *Mössbauer Reference and Data Index*, pp. 1966–1978. Plenum Press, New York